The Journal of Neuroscience, April 1, 1999, *19*(7):2609–2618

Differential Effects of Apamin- and Charybdotoxin-Sensitive K^+ Conductances on Spontaneous Discharge Patterns of Developing Retinal Ganglion Cells

Guo-Yong Wang, Bruno A. Olshausen, and Leo M. Chalupa

Section of Neurobiology, Physiology, and Behavior and the Center for Neuroscience, University of California, Davis, Davis, California 95616

The spontaneous discharge patterns of developing retinal ganglion cells are thought to play a crucial role in the refinement of early retinofugal projections. To investigate the contributions of intrinsic membrane properties to the spontaneous activity of developing ganglion cells, we assessed the effects of blocking large and small calcium-activated potassium conductances on the temporal pattern of such discharges by means of patch-clamp recordings from the intact retina of developing ferrets. Application of apamin and charybdotoxin (CTX), which selectively block the small and large calcium-activated potassium channels, respectively, resulted in significant changes in spontaneous firings. In cells recorded from the oldest animals [postnatal day 30 (P30)–P45], which manifested relatively sustained discharge patterns, application of either blocker induced bursting activity. With CTX the bursts were highly periodic, short in duration, and of high frequency. In contrast, with apamin the interburst intervals were longer, less regular, and lower in overall spike frequency. These differences between the effects of the two blockers on spontaneous activity were documented by spectral analysis of discharge patterns. Filling cells from which recordings were made with Lucifer yellow revealed that these effects were obtained in all three morphological classes of cells: α, β, and γ. These findings provide the first evidence that apamin- and CTX-sensitive K^+ conductances can have differential effects on the spontaneous discharge patterns of retinal ganglion cells. Remarkably, the bursts of activity obtained after apamin application in more mature neurons appeared very similar to the spontaneous bursting patterns observed in developing neurons. These findings suggest that the maturation of calcium-activated potassium channels, particularly the apamin-sensitive conductance, may contribute to the changes in spontaneous firings exhibited by retinal ganglion cells during the course of normal development.

Key words: retinal ganglion cells; spontaneous activity; apamin; CTX; Ca-mediated K^+ channels; patch-clamp recordings; development

Developing neurons in many different systems exhibit pronounced changes in their excitable membrane properties (Llinás, 1988; Spitzer, 1991; Ramoa and McCormick, 1994; Robinson and Wang, 1998). Retinal ganglion cells have provided a particularly attractive model for such studies (for review, see Chalupa, 1995) because the activity of these neurons is thought to play a key role in the refinement of early projection patterns at retinorecipient nuclei, even before birth (Galli and Maffei, 1988; Maffei and Galli-Resta, 1990; Meister et al., 1991; Skaliora et al., 1993; Wong et al., 1993; Wong and Oakley, 1996; Penn et al., 1998).

To gain a better understanding of the functional development of ganglion cells in the mammalian retina, we have made patch-clamp recordings from isolated and intact neurons with the goal of relating increases in excitability to the maturation of specific membrane conductances (Skaliora et al., 1993, 1995; Wang et al., 1997; Huang and Robinson, 1998). This work has revealed that an increase in sodium current density, as well as shifts in the kinetics of sodium channel activation and inactivation, accounts for the ability of ganglion cells to generate spikes very early in development (Skaliora et al., 1993). The ability to fire repetitive spikes to maintain depolarizing current injections, at later stages of development, has been related to an increase in the speed of recovery from sodium channel inactivation (Wang et al., 1998).

The spontaneous activity patterns of retinal ganglion cells have also been shown to exhibit pronounced developmental changes (Meister et al., 1991; Wong et al., 1993; Wong and Oakley, 1996; Zhou, 1998; the present study). Early in development, ganglion cells only fire occasional bursts, whereas at maturity, these cells typically manifest relatively sustained discharge patterns, with little or no bursting activity. The underlying basis for such changes in spontaneous activity with development are unknown, but it seems reasonable to think that both extrinsic as well as intrinsic factors are involved in this maturational process. With respect to extrinsic influences, recent studies have implicated GABAergic inputs (Fischer et al., 1998) as well as cholinergic starburst amacrine cells (Feller et al., 1996; Zhou, 1998) in the changing spontaneous activity patterns exhibited by developing ganglion cells. As yet, however, the involvement of specific conductances in the generation of different patterns of spontaneous activity has not been examined in the developing or adult retina.

Recently, we showed that ganglion cells in the ferret retina express two types of calcium-sensitive potassium conductances, corresponding to the large-conductance calcium-activated potassium channel (BK_{Ca}) and the small-conductance calcium-activated potassium channel (SK_{Ca}) (Wang et al., 1998). Both channels were found to modulate the evoked-activity patterns of retinal ganglion cells because application of apamin, the small-

Received Nov. 12, 1998; revised Jan. 13, 1999; accepted Jan. 20, 1999.

This work was supported by the National Eye Institute of the National Institutes of Health Grant EY03991. We thank Drs. Andrew T. Ishida, Joel E. Keizer, Martin Wilson, and Bogdan Dreher for their comments on this manuscript.

Correspondence should be addressed to Dr. Leo M. Chalupa, Section of Neurobiology, Physiology, and Behavior, University of California, Davis, Davis, CA 95616.

 0270-6474/99/192609-10$05.00/0

conductance channel blocker, and charybdotoxin (CTX), the large-conductance channel blocker, resulted in significant increases in discharge rates in response to injected currents. To assess the functional properties of these conductances further, we examined in the present study the effects of these two calcium-activated channel blockers on the spontaneous discharge patterns of ferret ganglion cells.

Here we show that the relatively sustained spontaneous firings observed in mature ganglion cells shift to a bursting mode when these calcium-activated potassium conductances are blocked. We also demonstrate clear-cut differences between the types of bursting activities elicited after application of the two blockers. Apamin, the small-conductance channel blocker, induced low-frequency bursts of relatively long duration, a pattern very similar to that observed in developing ganglion cells. In contrast, CTX, the large-conductance channel blocker, induced high-frequency bursts of short duration that were highly periodic. These findings demonstrate that modulations of calcium-activated potassium conductances provide an effective means for influencing the spontaneous discharge patterns of retinal ganglion cells. Moreover, because the firing patterns evident after blockade of the small conductance resembled the spontaneous discharges evident during development, the results suggest a possible link between the functional state of the calcium-activated potassium conductances and the spontaneous discharges manifested by immature ganglion cells. It remains to be established whether these effects are mediated by a direct influence on retinal ganglion cells or indirectly by amacrine cells that might also express calcium-activated potassium conductances.

MATERIALS AND METHODS

The preparation of the retina and the recording procedures have been described in detail in previous studies from this laboratory (Robinson and Chalupa, 1997; Wang et al., 1997, 1998). Here we emphasize that all procedures were in compliance with National Institutes of Health guidelines and were approved by the campus animal use committee.

Retina preparation. Retinas were obtained from ferrets ranging in age from postnatal day 15 (P15) to P45, with the day of birth denoted as P0. The animals were purchased from a commercial breeder (Marshall Farm, North Rose, NY). After the postnatal ferrets were given a lethal dose of barbiturate (Nembutal; 200 mg/kg, i.p.), the eyes were removed and placed in oxygenated Eagle's minimal essential medium (EMEM; Sigma M-7278, St. Louis, MO) at 25°C. The retinas were then carefully peeled from the eyecup and stored at room temperature in EMEM, continuously bubbled with 95% oxygen and 5% CO_2. A small piece of retina was placed, ganglion cell layer up, in the recording chamber and stabilized with an overlying piece of filter paper. A 2 mm hole in the filter paper provided access for the recording electrode. Cells were visualized through this opening with a 40× objective mounted on a fixed-stage upright epifluorescence microscope (Nikon) equipped with a mercury vapor lamp. The dissection of the retina and the recordings were done in an illuminated room so the retinas were under light-adapted conditions.

During recordings the retina was perfused continuously with EMEM (1.5 ml/min) through a gravity-fed line, heated with a Peltier device, and continuously bubbled with 95% oxygen and 5% CO_2. A calibrated thermocouple monitored the temperature in the recording chamber that was maintained at 35°C. Recordings from individual cells usually lasted 30–120 min, and retinal segments from which recordings were made typically remained viable for 8–12 hr. Patch electrodes were filled with a solution containing 140 mM KCl, 10 mM HEPES, 0.5 mM EGTA, 150 mg/ml Nystatin, 200 mg/ml Pluronic, and 2% Lucifer yellow, pH 7.4. By the end of the experiment the soma and the dendritic arborizations were usually completely labeled, suggesting that recordings were made in the whole-cell configuration. In some cases complete filling required additional application of a hyperpolarizing potential (200 mV) for ~5 min. After adequate filling was achieved, the retina was removed and fixed in 4% paraformaldehyde for 6–8 hr at 4°C. The retina, with filter paper still attached, was then mounted on a slide, and labeled cells were subsequently viewed with a Bio-Rad MRC-600 confocal microscope (Hercules, CA) and reconstructed using a computerized imaging system (Bio-Rad CoMOS, version 7.0) (Wang et al., 1997). Because withdrawal of the patch-clamp electrode sometimes distorted the shape of the soma, such reconstructions could not be made for all recorded cells. All cells were visualized and identified as ganglion cells before the electrode was withdrawn, and only cells unequivocally identified as retinal ganglion cells (Wingate et al., 1992) were included in this study.

Electrophysiology. Patch pipettes with a tip resistance between 3 and 7 MΩ were pulled from thick-walled 1.5-mm-outer-diameter borosilicate glass on a Sutter puller (P-87). Current-clamp recordings were made with an Axopatch 1-D patch-clamp amplifier. The data were low-pass filtered at rates between 1 and 2 kHz and digitized at rates between 1 and 4 kHz before storage on an IBM computer for subsequent off-line analysis. Recordings were obtained by patching onto cells with clear, nongranular cytoplasm. High-resistance seals were obtained by moving the patch electrode onto the cell membrane and applying gentle suction. After formation of a high-resistance seal between the electrode and the cell membrane, transient currents caused by pipette capacitance were electronically compensated by the circuit of the Axopatch 1-D amplifier. If the seal resistance dropped below 1 GΩ during the recording, the experiment was terminated.

The series resistance was 8–15 MΩ. Immediately after the whole-cell configuration was attained, the resting membrane potential was read off the amplifier. The value of the resting potential was monitored regularly throughout the recording, and if significant changes were observed, recordings were terminated. Apamin (1 μM) and CTX (0.02 μM) were freshly made on the day of the experiment and administered to the bath through a gravity-fed line. The high affinity of apamin and CTX for their respective channels made it difficult to wash out the drug, so only partial recovery toward control values could be obtained.

Analysis. The recorded activity was analyzed in terms of its frequency content by filtering each membrane potential waveform through a bank of bandpass filters evenly spaced along the log frequency axis (see Fig. 6*A*). The log frequency axis was used because of the large dynamic range in frequency and also because the power spectrum of the spiking activity indicated that energy is spread in progressively wider bands at higher frequencies. The bank consisted of 50 filters, each with a bandwidth of one-fifth octave (with Gaussian roll-off), and the center frequencies of the filters were uniformly spaced along the log frequency axis from 0.1 to 100 Hz. This allowed a large range of frequencies to be covered while at the same time allowing resolution of the sharpest frequency peaks observed in the power spectrum. The overall response of each filter was computed by summing the power (squared output) measured through each filter over time, normalizing these quantities across frequency, and then taking the square root as a measure of "amplitude." That is, for a recorded waveform $s(t)$, the output of the ith filter was obtained by convolving with filter $h_i(t)$:

$$s_i(t) = s(t) \otimes h_i(t),$$

where $h_i(t)$ has the frequency response:

$$h_i(f) = e^{-\frac{(f-f_{0i})^2}{2\sigma^2}}$$

$$\sigma = \frac{1}{2}\frac{\mathrm{BW_{oct}}}{\sqrt{\ln 2}}, \quad \mathrm{BW_{oct}} = 0.2,$$

and f_{0i} steps in uniform increments of one-fifth octave from 0.1 to 100 Hz. (Filtering was performed by multiplication in the frequency domain.) The overall response of the filter r_i was computed as:

$$r_i = \sqrt{\frac{p_i}{\sum_i p_i}}$$

$$p_i = \int s_i^2(t)dt.$$

Each recorded waveform was thus characterized by a 50 element spectral vector r, each element of which measures relative amplitude within a certain frequency band.

The recorded waveforms were analyzed for similarities and differences in their spectral characteristics before and after channel block by performing two forms of cluster analysis. The first method was primarily

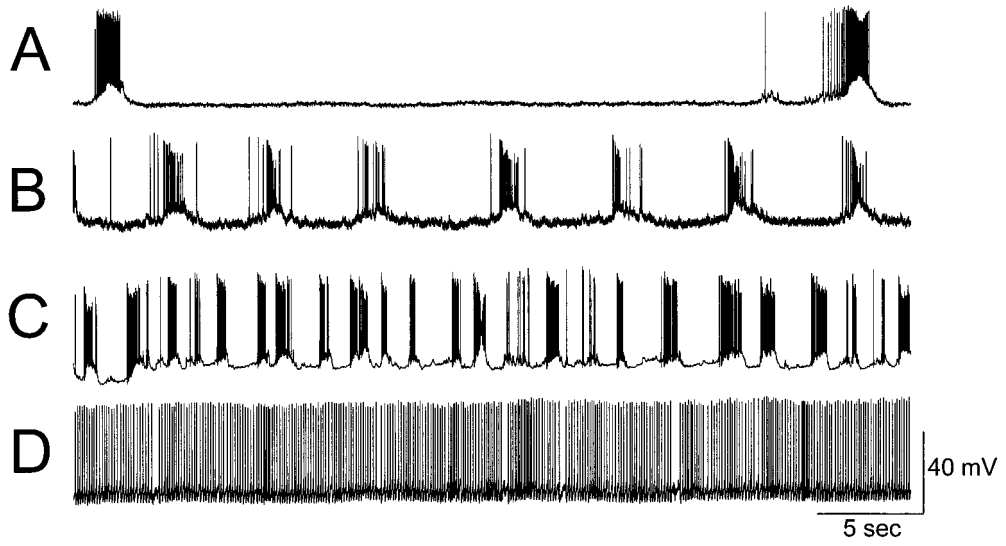

Figure 1. Current-clamp data obtained at body temperature from spontaneously active retinal ganglion cells at different stages of development. The ages of the four illustrative neurons are P17 (*A*), P26 (*B*), P35 (*C*), and P42 (*D*). There are clear age-related changes in spontaneous discharge patterns. *A*, The youngest cell fires in a bursting pattern with long interburst intervals. *B–D*, The interburst intervals are reduced progressively with development, with the oldest cell manifesting a relatively sustained discharge pattern. The resting potentials for these four cells were −54, −57, −61, and −59 mV, respectively.

visual and consisted of computing the principal components of the 50-dimensional space spanned by the entire population of spectral vectors (all recordings) and then projecting the spectral vector for each waveform α, $r^{(\alpha)}$, along the first two principal components. That is, a covariance matrix, C, of the total population of spectral vectors was calculated via:

$$C = \frac{1}{N}\sum_{\alpha}(r^{(\alpha)} - \mu)(r^{(\alpha)} - \mu)^T,$$

where N is the number of recordings, μ is the mean vector:

$$\mu = \frac{1}{N}\sum_{\alpha} r^{(\alpha)},$$

and α indexes the spectral vector measured for each recording. The principal components were obtained by calculating the eigenvectors of C:

$$Ce_i = \lambda_i e_i,$$

and a scatter plot was generated by projecting each frequency vector onto the first two eigenvectors (i.e., those with the largest eigenvalue):

$$v_1^{(\alpha)} = r^{(\alpha)} \cdot e_1$$

$$v_2^{(\alpha)} = r^{(\alpha)} \cdot e_2,$$

and plotting a point for each pair $[v_1{}^{(\alpha)}, v_2{}^{(\alpha)}]$. The second method provided a more quantitative measure of cluster separation by comparing the distance between cluster means with the within-cluster scatter. Because all spectral vectors were of unit length, the distance and scatter measures were based on the angle of separation between vectors. That is, a normalized mean vector for class j was calculated via:

$$\mu_j = \frac{1}{N_j}\sum_{i\in\Omega_j} r^{(i)}$$

$$\mu_j = \frac{\mu_j}{|\mu_j|};$$

where Ω_j is the set of indices in class j and N_j is the number of vectors in class j. The angular distance between means for classes i and j was calculated via:

$$\theta_{ij} = \cos^{-1}(\mu_i \cdot \mu_j),$$

and the within-class scatter for class j was calculated via:

$$\sigma_{\theta_j} = \frac{1}{N_j}\sum_{i\in\Omega_j} \cos^{-1}(r^{(i)} \cdot \mu_j).$$

RESULTS

Current-clamp recordings from morphologically identified retinal ganglion cells revealed marked developmental differences in spontaneous activity patterns (Fig. 1). In the youngest animals (P15–P19), ganglion cells (n = 3; resting potential, −54 ± 4.1 mV) fired action potentials in bursts of relatively long duration (4.7 ± 1.34 sec) separated by long intervals (43 ± 12 sec) of silence. In older retinas (P20–P26), the spontaneous bursts of ganglion cells (n = 4; resting potential, −55 ± 3.1 mV) decreased in duration (1.35 ± 0.14 sec), and the interval between bursts became substantially shorter (6.3 ± 2.7 sec). In the next age group (P30–P37), 22% of the cells (6 of 27) manifested a bursting pattern, with a burst duration and interburst interval of 1.04 ± 0.15 and 1.25 ± 0.10 sec, respectively (resting potential, −55.6 ± 4.9 mV), whereas the remainder of the neurons discharged in a relatively sustained manner (resting potential, −57.2 ± 5.3 mV). In contrast, in the oldest animals (P38–P45), all but one cell (27 of 28) fired in a relatively sustained pattern (resting potential, −57 ± 5.2 mV). Burst duration was measured from the beginning of the depolarization to the end of the repolarization period, and the interburst interval was measured from the end of one burst to the beginning of the subsequent burst. The data presented here are means ± SEs. In all cases, cells manifested a given spontaneous activity pattern (i.e., bursting or sustained) throughout the duration of the recording period that lasted from 30 min to as much as 2 hr.

By filling the neurons from which recordings were made with Lucifer yellow, it was possible to distinguish three major classes of ferret ganglion cells (α, β, and γ) on the basis of their salient morphological properties (Fig. 2). This was the case even in the youngest retinas studied (P15–P19). However, we did not distinguish between On and Off cell classes because, in our experience, it has proven problematic to localize accurately the dendritic processes of Lucifer yellow–filled neurons to these sublaminae of the inner plexiform layer.

At all ages, there was no obvious relationship between the different types of spontaneous discharge patterns observed (i.e., bursting or relatively sustained) and the morphological cell class. For instance, of the cells that fired in a sustained manner in animals older than P30, 10 were α, 17 were β, and 6 were γ. In this age group, the cells that discharged in a bursting manner were 1

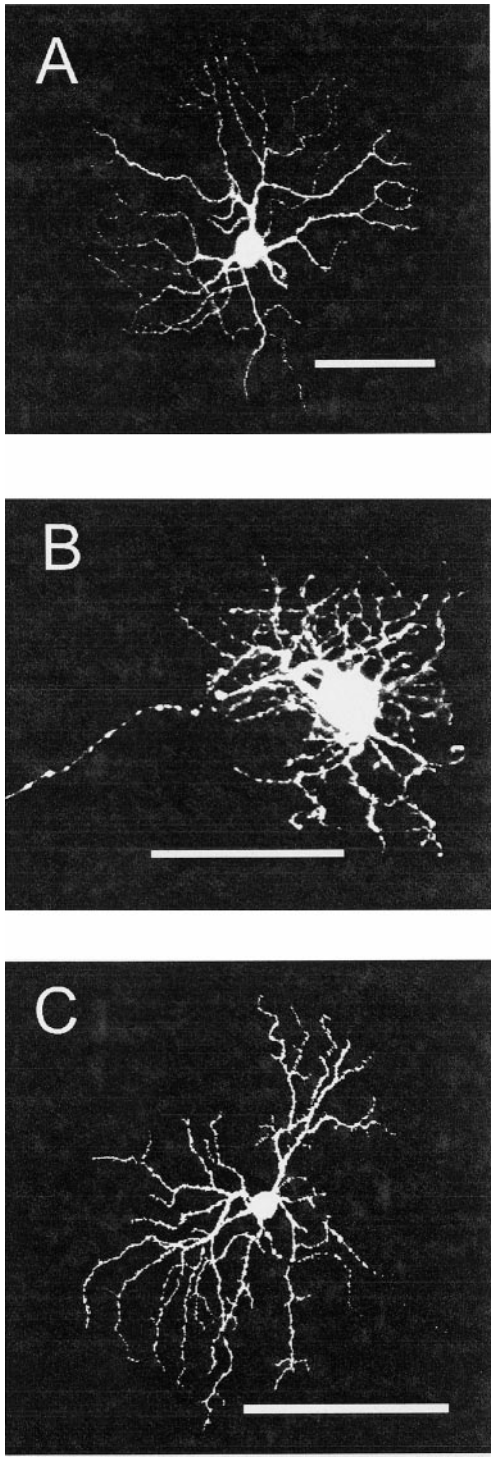

Figure 2. Confocal reconstructions of three morphological cell types from which recordings were made. *A–C*, An α cell (*A*), a β cell (*B*), and a γ cell (*C*), based on the criteria of Wingate et al. (1992). Ages of these cells were P39, P36, and P42, respectively. Cells were filled with Lucifer yellow during recordings. Scale bars: *A*, *C*, 100 μm; *B*, 50 μm.

α, 5 β, and 1 γ. At ages younger than P30, 7 cells were morphologically classified (1 α, 5 β, and 1 γ), and all showed bursting activity. These observations suggest that the different spontaneous patterns reflect the maturational state of these neurons rather than class-specific membrane properties. Note that the γ cell class may have included different subtypes of cells, but given the limited sample size, no attempt was made to distinguish cell classes further.

A total of 48 cells that manifested a sustained firing pattern (at P30 and older) were tested for the effects of one or the other calcium-activated potassium channel blocker. In the majority of cases the spontaneous discharges were significantly altered, and in all instances this was reflected in a shift from a maintained to a bursting pattern: 18 of 21 cells were affected by CTX, and 22 of 27 neurons were influenced by application of apamin. Examples of the effects obtained are depicted for two neurons in Figure 3. Note that both cells manifested relatively sustained levels of spontaneous activity before application of the drugs (Fig. 3, *left*). After introduction of apamin (Fig. 3*B*, *right*) or CTX (Fig. 3*A*, *right*), the spontaneous discharges changed to a bursting pattern. This type of change was evident in every cell tested whose firing pattern was affected by the drug treatment, and there was no indication of class-specific effects. Of the cells affected by apamin, 6 were α, 10 were β, and 3 were γ; and of those influenced by CTX, 4 were α, 7 were β, and 3 were γ. The number of morphologically identified cells is lower than that of the overall sample because in some cases the process of withdrawing the patch electrode altered cell morphology.

It is also evident in Figure 3 that the type of bursting activity obtained with CTX was different than that observed after apamin application. With CTX the interval between bursts was brief, and there were few spikes in each burst (Fig. 3*A*). In contrast, with apamin the interburst interval was longer, and the spike frequency in each burst was higher (Fig. 3*B*). The average duration of bursts and the interburst interval were 0.102 ± 0.025 and 0.200 ± 0.020 sec, respectively, (n = 18) for CTX and 1.198 ± 0.200 and 1.786 ± 0.224 sec, respectively, (n = 22) for apamin. The examples depicted in Figure 3 are representative of the results obtained for the overall sample of cells tested with the two blockers. Because the affinity for these blockers is high, it was not possible to test the effects of both drugs on a single cell. Nevertheless, the clear-cut differences between apamin and CTX were readily apparent in the sample of cells tested.

Particularly noteworthy is the observation that the bursting activity obtained after apamin application was very similar to that manifested by immature neurons. This finding is clearly illustrated in Figure 4 that compares the spontaneous discharge patterns, using the same time scale, recorded from two immature cells (Fig. 4*A*,*B*) and two more mature neurons (Fig. 4*C*,*D*) after apamin application. The two mature cells manifested a relatively sustained pattern (data not shown), but after apamin application the resulting bursts were found to be virtually indistinguishable from those observed in developing cells. Note that with apamin application there was also a positive shift in the baseline, indicating a partial depolarization of membrane potential that might reflect the influx of calcium during the bursting period (clearly evident in Figs. 3*B*, *right*, 4*C*). In contrast, the bursts obtained after CTX application were much more regular than those recorded in developing neurons.

To obtain a quantitative comparison of the effects of apamin and CTX, we performed spectral analyses on the waveform patterns recorded during the control condition and also after application of one or the other blocker for the cells that manifested sustained levels of spontaneous activity. In each condition, the recordings were analyzed for their frequency content in the range from 0.1 to 100 Hz, on a logarithmic frequency scale, as described in Materials and Methods. Representative illustrations of such an analysis for the two cells that provided the examples of

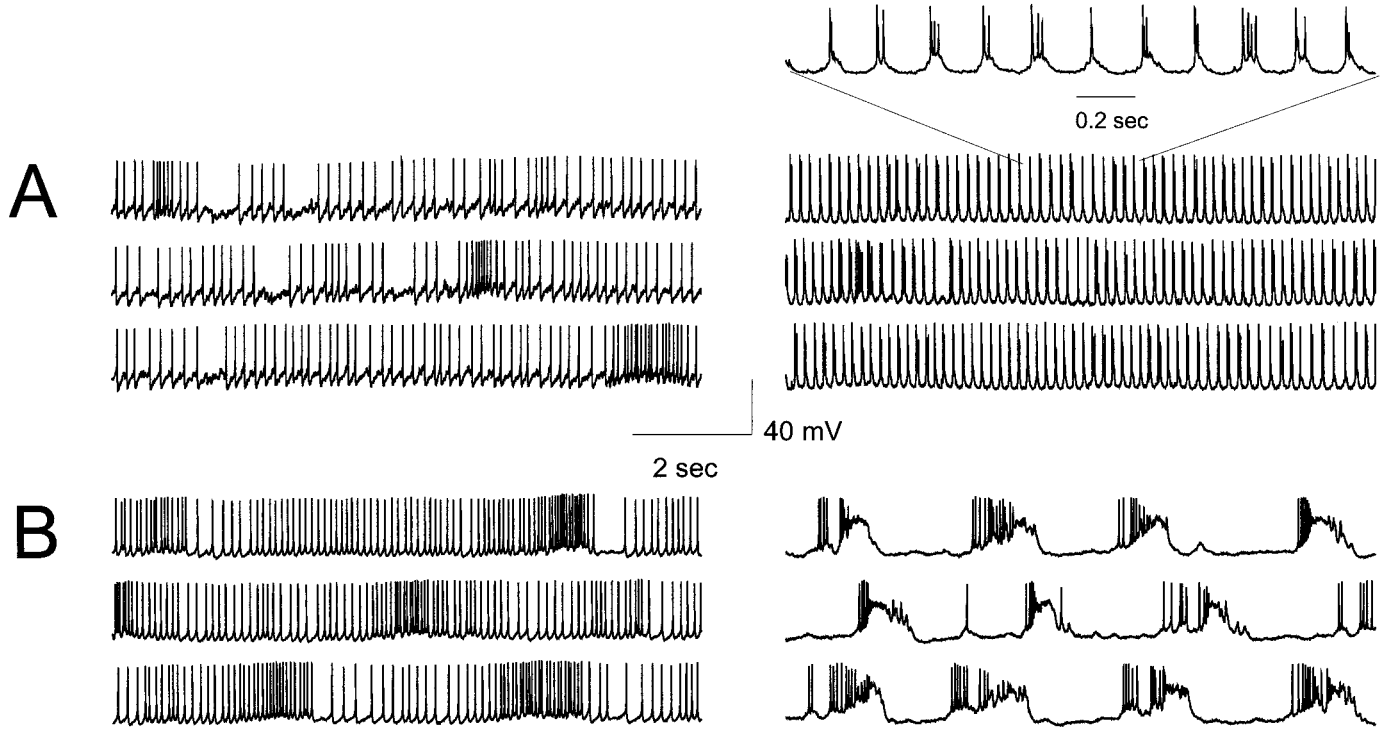

Figure 3. Current-clamp recordings at body temperature. *A*, *B*, The responses of two mature retinal ganglion cells that fired in a sustained pattern to bath application of charybdotoxin and apamin, the large and small calcium-activated potassium channel blockers, respectively. *Left*, The control recordings. *Right*, The recordings after bath application of the blockers. Both charybdotoxin and apamin induced bursting activity. With CTX the duration of bursts and the interburst intervals are short (*A*, *right*). In contrast, with apamin the duration of bursts and the interburst intervals are long (*B*, *right*). The average duration of bursts and the interburst interval are 0.076 ± 0.035 sec (n = 247 bursts) and 0.176 ± 0.042 sec (n = 236 intervals), respectively, for CTX and 1.153 ± 0.282 sec (n = 213 bursts) and 1.733 ± 0.221 sec (n = 197 intervals), respectively, for apamin. The age and the resting potential of these two cells were P38 and −56 mV (*A*) and P35 and −55 mV (*B*).

change in spiking patterns with each blocker (see Fig. 3) are depicted in Figure 5. In the control condition, there is a rather broad spread of energy in the range from 1 to 100 Hz, with the peak frequency corresponding to the spontaneous discharge rate of the cells. There is also a substantial peak in the low-frequency range (0.1–1 Hz), most likely attributable to slow modulations in firing rate. After application of one or the other blocker, there is a pronounced shift in the spectrum that is different for each blocker. Apamin tends to give rise to a strong low-frequency component in the 0.3–0.6 Hz range (Fig. 5*B*, *right*) corresponding to the long periodic bursts seen in Figure 3*B*, *right*. CTX, in contrast, gives rise to a sharply tuned peak at ~5 Hz (Fig. 5*A*, *right*) corresponding to the highly regular periodic bursting pattern seen in Figure 3*A*, *right*. In addition, for both blockers the overall activity as measured by the signal variance (proportional to the area under the power spectrum) is higher. Application of CTX resulted in a fivefold increase in variance for this cell, whereas application of apamin resulted in a 1.3-fold increase. Importantly, the basis for this increase in power was different for the two blockers. In the case of CTX there was a 2.5-fold increase in the total number of spikes emitted when the blocker was applied in comparison with the control condition (compare Fig. 3*A*, *right* and *left*). In contrast, with apamin application there was a 4.7-fold decrease in the total number of spikes, but the pronounced positive shift in the membrane potential during the emission of the bursts, in addition to the increased discharge rate during the bursts, resulted in the power increase (compare Fig. 3*B*, *left* and *right*).

To focus further on the temporal structure of the recordings obtained in the various conditions, we calculated the power in different frequency bands evenly spaced along the log frequency axis, as shown in Figure 6*A*, and normalized these quantities with respect to the total signal power as described in Materials and Methods. The changes obtained after apamin and CTX application are shown in a color-coded format in Figure 6*B*. The shift to low-frequency activity after application of apamin and to sharply tuned mid-frequency activity after application of CTX appears as a highly robust effect across the population of cells analyzed. Also shown (Fig. 6*B*, *bottom*) is the frequency spectrum of seven developing cells (P30–P42) that fired spontaneous bursts. Note that the frequency profiles of these neurons closely resemble those obtained after apamin application.

To characterize statistically the similarities and differences among the groups of cells studied, we constructed a two-dimensional scatter plot of all recorded waveforms. This was done by projecting the log frequency spectrum for each cell onto the first two principal components, accounting for 75% of the variance. The result of this analysis, shown in Figure 7*A*, depicts how activity patterns cluster into groups according to the frequency characteristics of their discharge patterns under the different experimental conditions. The change from control to apamin block is seen as a shift along the first principal component (Fig. 7*A*, *blue + symbols* changing to *blue ○ symbols*), whereas the shift from control to CTX block is seen as a shift along the second principal component (Fig. 7*A*, *red + symbols* changing to *red ○ symbols*). The group of immature cells (Fig. 7*A*, *green + symbols*) overlaps completely with the apamin group (Fig. 7*A*, *blue ○ symbols*). Figure 7*B* graphically depicts the results of a more

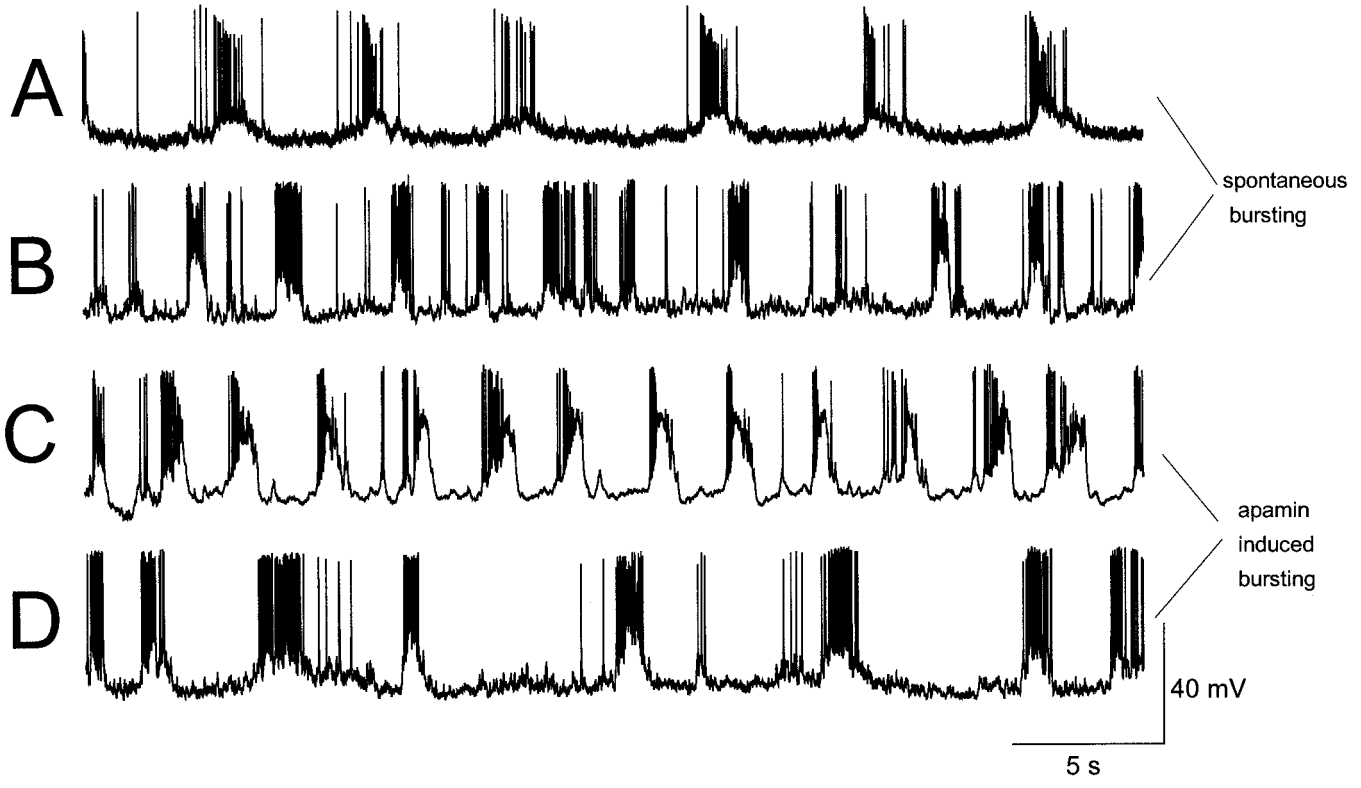

Figure 4. Current-clamp recordings from four retinal ganglion cells at body temperature. *A*, *B*, Spontaneous bursting activities of two cells at P26 and P31, respectively. *C*, *D*, Bursting activities induced by apamin from two older cells at P35 and P38, respectively, that manifested relatively sustained spontaneous discharge patterns (data not shown). Note that the bursting waveforms induced by apamin (*C*, *D*) are similar to those of spontaneous bursts observed in the less mature cells. Resting potentials of these four cells were −57 mV (*A*), −56 mV (*B*), −55 mV (*C*), and −57 mV (*D*).

quantitative analysis of the overlap and separation among the clusters corresponding to the different experimental conditions. The separation between clusters, calculated as the angular separation between the mean vector of each cluster (see Materials and Methods), is shown on the line connecting the dots corresponding to each experimental condition. The amount of within-cluster scatter is shown on the circle surrounding each dot. It is thus evident that the effects of apamin and CTX are significantly separated from their control conditions, as well as from each other, and that the immature group overlaps strongly with the apamin group.

DISCUSSION

In this study whole-cell patch-clamp recordings were made from morphologically identified ganglion cells in the intact retina of the developing ferret. During ontogeny spontaneous firing patterns were observed to change markedly. Early in development, ganglion cells fired in bursts separated by silent intervals that decreased with age. In contrast, in the oldest age group studied, all but one cell manifested a relatively sustained pattern of spontaneous activity. Similar observations have been reported by Wong and colleagues using multielectrode recordings (Wong et al., 1993) as well as Ca^{2+} imaging (Wong and Oakley, 1996) of the ferret retina. As yet, however, it is not know what accounts for such changes in spontaneous activity of retinal ganglion cells. This issue is of considerable importance because there is now convincing evidence that such bursts of activity could play a role in refining connections in developing retinogeniculate pathways (Meister et al., 1991; Wong et al., 1993; Wong and Oakley, 1996; Penn et al., 1998). Because isolated ganglion cells seldom yield spontaneous action potentials (Skaliora et al., 1993; see also Feigenspan et al., 1998), it seems reasonable to think that inputs from retinal interneurons are required for such activity. In support of this hypothesis, Zhou (1998) has recently found bursting type of activity in starburst amacrine cells of the developing ferret retina during the period when such activity is prevalent in ganglion cells.

In the present study we provide evidence that intrinsic membrane properties may also play a role in the spontaneous patterns generated by developing ganglion cells. Previously, we demonstrated that ferret retinal ganglion cells express two types of calcium-activated potassium conductances (Wang et al., 1998), with properties similar to those described for BK_{Ca} and SK_{Ca} channels documented in other neurons (e.g., Blatz and Magleby, 1987). Here we show that application of specific blockers of these channels has marked effects on spontaneous discharge rates. Cells that fired in a relatively sustained manner changed to bursting patterns when either the large or the small calcium-activated conductance was blocked. This was the case for α, β, and γ cells, the three major classes of ganglion cells identified after the neurons from which recordings were made were filled with Lucifer yellow.

Implication for developmental changes in spontaneous activity

When the small-conductance calcium-activated potassium channel was blocked by apamin in the older ferret retinas, the resulting firing patterns became bursty, resembling those observed in younger ganglion cells. This implies that there might be some functional equivalence between developing ganglion cells that

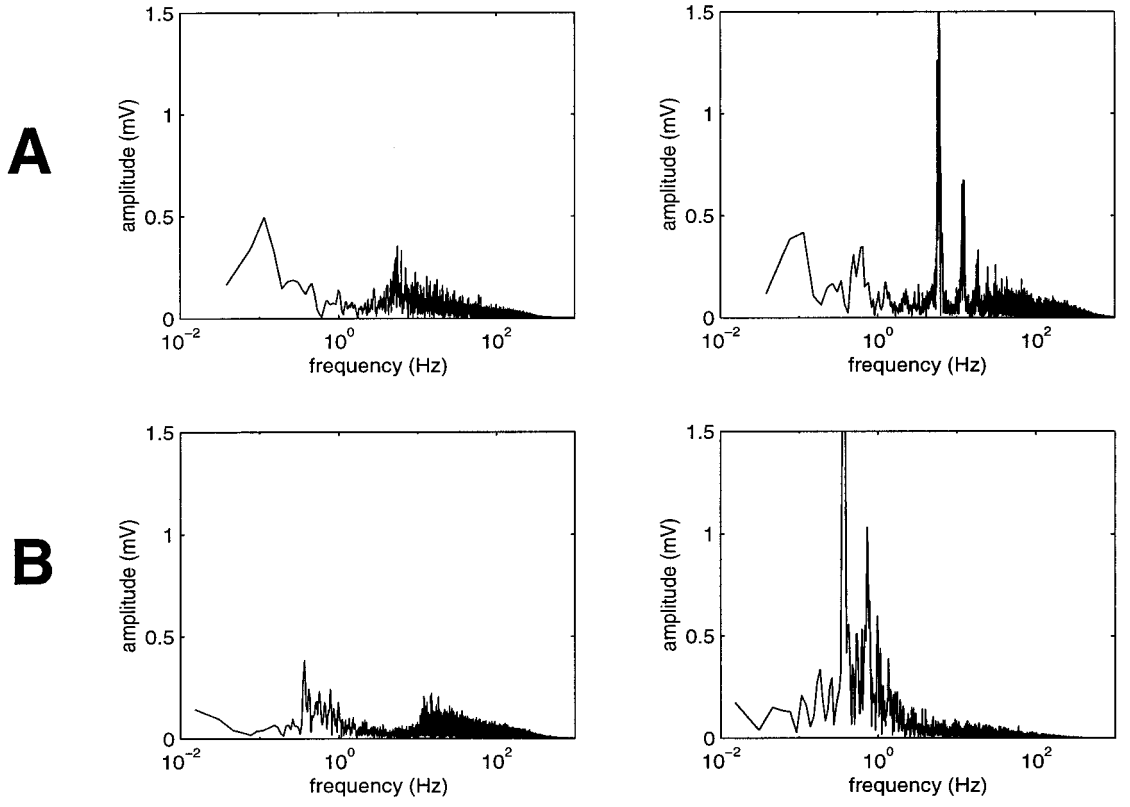

Figure 5. Amplitude spectra of the same spiking patterns shown in Figure 3 before (*left*) and after (*right*) block. *A*, CTX results in sharper tuning at ~5 Hz. *B*, Apamin results in a dominant frequency at ~0.3–0.6 Hz. In both cases there is an increase in the variance or total power in the recorded activity (revealed here as an increase in area under the amplitude spectrum).

discharged bursting patterns and the more mature neurons subjected to pharmacological blockade of the small calcium-activated potassium channel. One intriguing possibility is that the expression and functional maturation of this channel contribute to the changing patterns of spontaneous activity observed in developing ganglion cells. For instance, it might be the case that after this conductance attains a mature state, the capability to discharge bursts to a given synaptic input is lessened. One test of this idea would be to examine the functional maturation of this calcium-activated conductance in relation to changes in spontaneous discharges manifested by developing neurons.

Undoubtedly other factors must contribute to this process, and indeed, there is now accumulating evidence of maturational changes in the properties and kinetics of a diversity of currents expressed by developing ganglion cells (for review, see Robinson and Wang, 1998). Specifically, we have shown that the speed of recovery from inactivation of the Na current increases markedly with ganglion cell development and that this relates to the ability of these neurons to generate repetitive firing patterns (Wang et al., 1997). That study and the previous work from our laboratory on the functional development of intrinsic membrane properties of ganglion cells in the developing mammalian retina (Skaliora et al., 1993) were primarily concerned with discharge patterns generated by depolarizing current injections. In contrast, in the present study we focused on the spontaneous activity patterns of developing retinal ganglion cells. To assess further the relative contributions of the diverse conductances to the functional maturation of ganglion cells will require the formulation of a quantitative model, and such work is now in progress (Benison et al., 1997).

Distinct functional role of small and large K_{Ca} channels

Application of both apamin and CTX significantly altered spontaneous activities of retinal ganglion cells by changing relatively sustained rates to bursting-type patterns. At the same time, there were significant differences between the types of bursts observed after application of the two blockers. When the large-conductance calcium-activated potassium channel was blocked by CTX, the discharges became highly regular with brief periodic bursts separated by relatively short intervals, typically <200 msec apart. In contrast, blockade of the small-conductance calcium-activated potassium channel by application of apamin resulted in longer periodic bursts separated by longer periods of inactivity. This distinction between the actions of the two blockers, first apparent in individual recordings, was confirmed by comparisons of the frequency spectra obtained after applications of one or the other blocker. These findings provide the first evidence of a functional distinction between the large and small calcium-activated potassium channels in regulating the spontaneous discharges patterns of retinal ganglion cells. The underlying basis for the differential effects of apamin and CTX on spontaneous discharge patterns of retinal ganglion cells remains to be established. Recently, microinjections of apamin and CTX into the rat's inferior olive have been shown to have different effects on the generation of rhythmicity of complex spikes in Purkinje neurons of the cerebellum (Lang et al., 1997). Thus, the two calcium-activated conductances may have differential roles in the generation of rhythmic activity in diverse neural systems.

As discussed above, the similarity in the bursting patterns evident after apamin application and in the spontaneous bursts

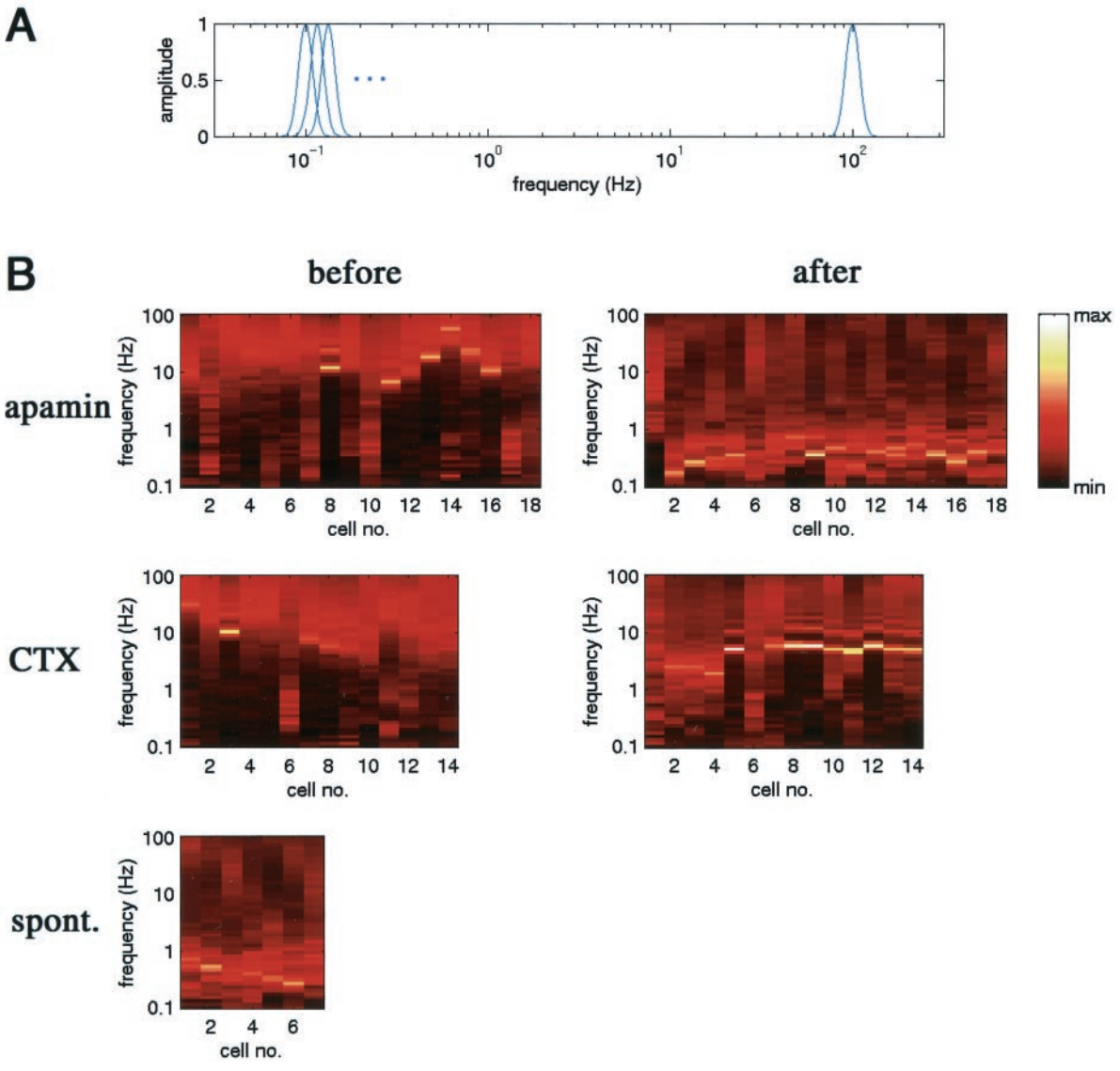

Figure 6. Log frequency spectra for the cells recorded before and after apamin or *CTX* application as well as for those showing spontaneous (*spont.*) bursting activity. *A*, Spectra were computed by filtering through a bank of 50 filters, each one-fifth octave in bandwidth and spaced evenly along the log frequency axis from 0.1 to 100 Hz. Shown are the frequency response functions of the first three and last of these filters (the *horizontal dots* represent the repetition of the filters at equally spaced intervals along the log-frequency axis). *B*, Normalized spectra are displayed as "heat maps," in which the amplitude in each frequency band is displayed with a color corresponding to the fraction of signal energy falling within that band. (*Red–white* is strongest, and *black* is weakest.) Each *column* corresponds to the spectrum for an individual cell, with frequency increasing logarithmically from *bottom* to *top*. In the control condition (before), the signal energy is clustered in the range from 10 to 100 Hz, corresponding to the spontaneous firing rates of these cells. After apamin is applied, there is a pronounced shift to lower frequencies, whereas after *CTX* is applied, there is a pronounced sharpening at ~5 Hz. The normalized spectrum of the group of cells that manifested spontaneous bursts of activity shows the same low-frequency trend seen in the apamin group. Note that the number of cells used in this analysis is lower than that of the overall sample studied because some recordings were too brief in duration to be useful for Fourier analysis.

generated by developing neurons implies that the maturation of the small-conductance calcium-mediated channel may be implicated in the developmental changes in activity manifested by these neurons. In contrast, the type of spontaneous activity evident in ganglion cells after CTX application would seem to be much more rhythmic than that observed under "normal conditions" in either the developing or mature retina. Consequently, the putative role of the large-conductance calcium-mediated potassium channel in the generation of these highly rhythmic discharge patterns is unclear, at present. One possibility is that this channel always works in combination with a variety of other conductances to alter spontaneous discharges so that the type of activity observed after selectively blocking this channel may not occur naturally. Alternatively, such patterns might be present during a delimited developmental period or under specific conditions at maturity.

Direct or indirect influence of the blockers?

In the present study recordings were made from the intact retina, and consequently, we cannot identify the site of action of the calcium-activated potassium channel blockers we used. In a previous study, we showed by means of single-channel recordings from isolated neurons that ferret ganglion cells express both small-conductance and large-conductance calcium-activated po-

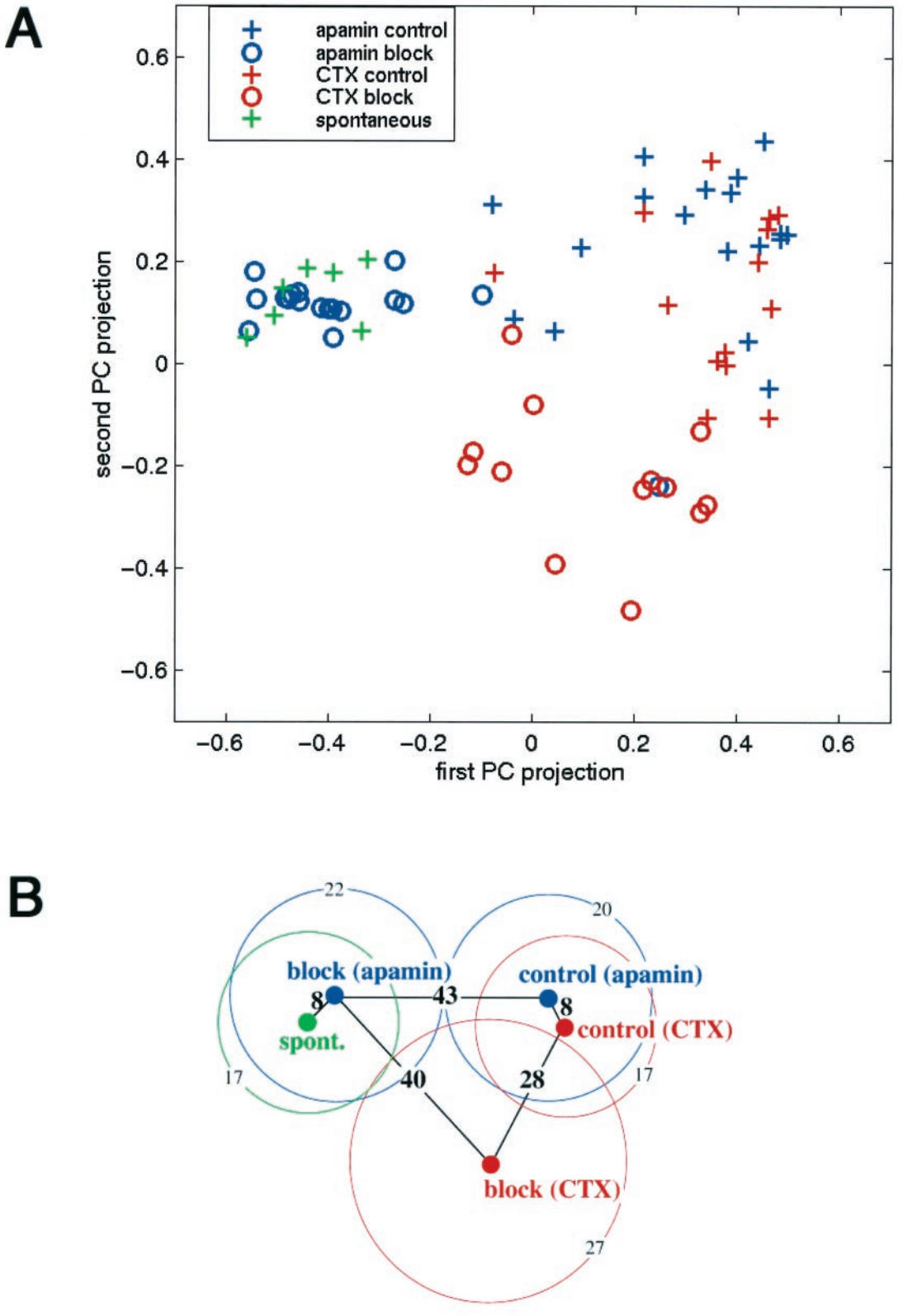

Figure 7. Clustering of the cells according to their firing patterns. *A*, The normalized spectra were projected onto the first two principal components of the 50-dimensional log frequency space of all the cells tested. The change in activity attributable to apamin block (*blue*) results in a shift along the first principal component, whereas the change in activity attributable to *CTX* block (*red*) results in a shift along the second principal component. The spontaneous group (*green*) overlaps with the apamin group. *B*, A graphical depiction of between-class separation in comparison with within-class scatter is shown. Each *dot* denotes a different experimental condition, and the *lines connecting dots* denote the angular separation between cluster means (see Materials and Methods). The *circle around* each *dot* denotes the degree of within-class scatter that is given quantitatively on the circumference. The firing patterns elicited by apamin and *CTX* are well separated from that of their controls and of each other, whereas the cells that manifested spontaneous bursts of activity show little or no significant separation from the apamin group.

tassium channels (Wang et al., 1998). Thus, one distinct possibility is that the effects documented in the present study on the spontaneous discharge patterns were caused by the direct influence of apamin and CTX on the small-conductance and large-conductance calcium-activated potassium channels present in the membrane of ferret ganglion cells. Another possibility is that the effects of apamin and CTX, described here, reflected the actions of these drugs on retinal interneurons and, in particular, on starburst amacrine cells that have been implicated in driving the slow-bursting activity found in young ferret ganglion cells (Feller et al., 1996; Zhou, 1998). Although calcium-activated potassium channels have been found in amacrine cells of the salamander retina (Eliasof et al., 1987), to our knowledge, the presence of such channels remains to be established in the interneurons of the ferret retina. It could also be the case that multiple cell types could contribute to the findings described here. Assessing the validity of these alternatives will be difficult because, as indicated previously, isolated ganglion cells rarely manifest spontaneous discharges and, consequently, it is not feasible to examine directly the effects of these channel blockers on such discharges in these neurons. Nevertheless, it seems reasonable to think that in the intact retina what is commonly termed "spontaneous" activity reflects synaptic activation as well as the intrinsic membrane conductances. The results of the present study, in conjunction with our previous work (Wang et al., 1998), indicate that modulation of large and small calcium-activated potassium channels could substantially alter evoked discharges as well as spontaneous activity patterns in mammalian retinal ganglion cells. More specifically, we have shown here that the state of the calcium-activated potassium channels could be crucially involved in the generation of spontaneous discharge patterns that have been linked with the activity-mediated refinements observed in the developing visual system.

Effects of spontaneous and evoked discharges are different

Mature retinal ganglion cells respond to depolarizing current injections with sustained discharge patterns for the duration of the stimulus (Skaliora et al., 1993; Wang et al., 1997, 1998). When such current injections were used to elicit spike discharges in ferret ganglion cells, application of both the large and the small calcium-activated potassium channel blocker produced a significance increase in spike frequency, without changing the overall discharge pattern (Wang et al., 1998). This was the case when recordings were made from isolated retinal ganglion cells as well as from ganglion cells in the intact retina. In contrast, as discussed above, application of apamin and CTX resulted in pronounced changes in spontaneous activity, and the resulting patterns were different after application of the two blockers. Collectively, these observations underscore a fundamental distinction between the mechanisms underlying spike generation when depolarizing current injections are used and those mediating spontaneous discharge patterns. One implication of these observations is that modulation of the calcium-activated potassium channels could act to alter photically evoked responses and spontaneous activity in fundamentally different ways in retinal ganglion cells of the behaving animal.

REFERENCES

Benison G, Keizer J, Robinson DW (1997) Model of the functional properties of postnatal cat retinal ganglion cell. Soc Neurosci Abstr 23:1025.

Blatz AL, Magleby KL (1987) Calcium-activated potassium channels. Trends Neurosci 10:463–467.

Chalupa LM (1995) The nature and nurture of retinal ganglion cell development. In: The cognitive neurosciences (Gazzaniga MS, ed), pp 37–50. Cambridge, MA: MIT.

Eliasof S, Barnes S, Werblin F (1987) The interaction of ionic currents mediating single spike activity in retinal amacrine cells of the tiger salamander. J Neurosci 7:3512–3524.

Feigenspan A, Gustincich S, Bean BP, Raviola E (1998) Spontaneous activity of solitary dopaminergic cells of the retina. J Neurosci 18:6776–6789.

Feller MB, Wellis DP, Stellwagen D, Werblin FS, Shatz CJ (1996) Requirement for cholinergic synaptic transmission in the propagation of spontaneous retinal waves. Science 272:1182–1187.

Fischer KF, Lukasiewicz PD, Wong RO (1998) Age-dependent and cell class-specific modulation of retinal ganglion cell bursting activity by GABA. J Neurosci 18:3767–3778.

Galli L, Maffei L (1988) Spontaneous impulse activity of rat retinal ganglion cells in prenatal life. Science 242:90–91.

Huang SJ, Robinson DW (1998) Activation and inactivation properties of voltage-gated calcium currents in developing cat retinal ganglion cells. Neuroscience 85:239–247.

Lang EJ, Sugihara I, Llinás R (1997) Differential roles of apamin- and charybdotoxin-sensitive K^+ conductances in the generation of inferior olive rhythmicity *in vivo*. J Neurosci 17:2825–2838.

Llinás RR (1988) The intrinsic electrophysiological properties of mammalian neurons: insights into central nervous system function. Science 242:1654–1664.

Maffei L, Galli-Resta L (1990) Correlation in the discharges of neighboring rat retinal ganglion cells during prenatal life. Proc Natl Acad Sci USA 87:2861–2864.

Meister M, Wong RO, Baylor DA, Shatz CJ (1991) Synchronous bursts of action potentials in ganglion cells of the developing mammalian retina. Science 252:939–943.

Penn AA, Riquelme PA, Feller MB, Shatz CJ (1998) Competition in retinogeniculate patterning driven by spontaneous activity. Science 279:2108–2112.

Ramoa AS, McCormick DA (1994) Developmental changes in electrophysiological properties of LGNd neurons during reorganization of retinogeniculate connections. J Neurosci 14:2089–2097.

Robinson DW, Chalupa LM (1997) The intrinsic temporal properties of alpha and beta retinal ganglion cells are equivalent. Curr Biol 7:366–374.

Robinson DW, Wang GY (1998) Development of intrinsic membrane properties in mammalian retinal ganglion cells. Semin Cell Dev Biol 9:301–310.

Skaliora I, Scobey RP, Chalupa LM (1993) Prenatal development of excitability in cat retinal ganglion cells: action potentials and sodium currents. J Neurosci 13:313–323.

Skaliora I, Robinson DW, Scobey RP, Chalupa LM (1995) Properties of K+ conductances in cat retinal ganglion cells during the period of activity-mediated refinements in retinofugal pathways. Eur J Neurosci 77:1558–1568.

Spitzer NC (1991) A developmental handshake: neuronal control of ionic currents and their control of neuronal differentiation. J Neurobiol 22:659–673.

Wang GY, Ratto G, Bisti S, Chalupa LM (1997) Functional development of intrinsic properties in ganglion cells of the mammalian retina. J Neurophysiol 78:2895–2903.

Wang GY, Robinson DW, Chalupa LM (1998) Calcium-activated potassium conductances in retinal ganglion cells of the ferret. J Neurophysiol 79:151–158.

Wingate RJ, FitzGibbon T, Thompson ID (1992) Lucifer yellow, retrograde tracers, and fractal analysis characterise adult ferret retinal ganglion cells. J Comp Neurol 323:449–474.

Wong RO, Oakley DM (1996) Changing patterns of spontaneous bursting activity of on and off retinal ganglion cells during development. Neuron 16:1087–1095.

Wong RO, Meister M, Shatz CJ (1993) Transient period of correlated bursting activity during development of the mammalian retina. Neuron 11:923–938.

Zhou ZJ (1998) Direct participation of starburst amacrine cells in spontaneous rhythmic activities in the developing mammalian retina. J Neurosci 18:4155–4165.